www.ksmrm.org JKSMRM 16(1) : 6-15, 2012
Print ISSN 1226-9751

Original Article

Background Gradient Correction using Excitation Pulse Profile for Fat and T_2* Quantification in 2D Multi-Slice Liver Imaging

Yoonho Nam[1], Hahnsung Kim[1], Sang-Young Zho[1], Dong-Hyun Kim[1, 2]
[1]Department of Electrical and Electronic Engineering, Yonsei University
[2]Department of Radiology, Yonsei University

Purpose : The objective of this study was to develop background gradient correction method using excitation pulse profile compensation for accurate fat and T_2* quantification in the liver.

Materials and Methods: In liver imaging using gradient echo, signal decay induced by linear background gradient is weighted by an excitation pulse profile and therefore hinders accurate quantification of T_2* and fat. To correct this, a linear background gradient in the slice-selection direction was estimated from a B_0 field map and signal decays were corrected using the excitation pulse profile. Improved estimation of fat fraction and T_2* from the corrected data were demonstrated by phantom and in vivo experiments at 3 Tesla magnetic field.

Results: After correction, in the phantom experiments, the estimated T_2* and fat fractions were changed close to that of a well-shimmed condition while, for in vivo experiments, the background gradients were estimated to be up to approximately 120 μT/m with increased homogeneity in T_2* and fat fractions obtained.

Conclusion: The background gradient correction method using excitation pulse profile can reduce the effect of macroscopic field inhomogeneity in signal decay and can be applied for simultaneous fat and iron quantification in 2D gradient echo liver imaging.

Index words : Fat quantification · T_2* measurement · IDEAL · field inhomogeneity · pulse profile · liver imaging

INTRODUCTION

Fatty infiltration of liver is one of the primary features of non-alcoholic fatty liver disease (NAFLD). Hepatic iron overload is also common in many liver diseases. Accurate quantification of the liver fat and iron content is an important factor in detecting hepatic diseases. Liver biopsy has been used for diagnosis of NAFLD, but the use of biopsy has problems such as invasiveness and sampling error. On the contrary, MRI is an efficient noninvasive tool for diagnosis of NAFLD (1, 2). Fat signal fraction can be estimated from chemical shift based multi-echo methods (3, 4) because the chemical shift between water and fat is large enough to separate (about 420Hz at 3.0T). Hepatic iron concentration can be estimated by T_2* measurements because iron overload accelerates T_2* decay (5, 6).

A recently developed chemical shift based method, named iterative decomposition of water and fat with echo asymmetry and least squares estimation (IDEAL), provides robust separation of water and fat signal with flexible echo sampling times (7). "T_2*-IDEAL" which is based on the IDEAL technique

• Received; February 22, 2012 • Revised; April 6, 2012
• Accepted; April 13, 2012
Corresponding author : Dong-Hyun Kim, Ph.D., Department of Electrical and Electronic Engineering, Yonsei University, 134 Shinchon-dong, Seodaemun-gu, Seoul 120-749, Korea.
Tel. 82-2-2123-5874, Fax. 82-2-313-2879
E-mail : donghyunkim@yonsei.ac.kr

provides T_2* measurements as well as water-fat decomposition using complex field map (8). Therefore, T_2*-IDEAL allows simultaneous quantification of fat and iron in liver with consideration of local B_0 field inhomogeneity.

T_2* decay in gradient echo imaging is not only affected by iron overload, but also by macroscopic field inhomogeneities induced by magnetic field imperfections or susceptibility differences at air-tissue boundaries. This artificial signal decay due to macroscopic field inhomogeneities should be considered because it may disturb accurate quantification. Generally, the scale of macroscopic field inhomogeneities induced by magnetic field imperfections or air-tissue boundaries is larger than the imaging voxel size while that of field inhmogeneities due to iron overload is smaller than the imaging voxel size. In typical 2D liver imaging, the voxel size in the slice-selection direction (i.e., a slice thickness) is larger than that of the in-plane direction. Thus, the effect of macroscopic field inhomogeneities can be approximated by a linear background gradient in the slice-selection direction. Several methods such as reducing the voxel size (9), estimating k-space trajectory (10) or using the tailored RF pulses (11) have been suggested to correct this type of an unwanted signal decay. Post-processing techniques using a sinc correction which assume a perfect rectangular slice profile, are effective because it doesn't require additional scan time or sequence modification (12, 13). However, the excitation pulse profile and the slice profile have Fourier relationship only when a small flip angle is applied. Signal decay due to linear background gradient is weighted by the time profile of the excitation pulse which is a function of both time and background gradient values (12, 14). Therefore, in reality, the decay depends on the excitation profile the RF pulse used.

In this study, we examine the effect of linear background gradient on fat and T_2* quantification in 2D liver imaging and present a correction algorithm using the excitation pulse profile. The correcting algorithm for linear background gradient is applied to T_2*-IDEAL algorithm and demonstrated by phantom and in vivo experiments.

MATERIALS AND METHODS

Signal Model

In the presence of linear background gradient, the signal from a voxel including water and fat in 2D gradient echo images can be represented as (8, 12):

$$s(t) = (w + f\, e^{\,i2\pi \Delta f t})\, e^{\,i2\pi \psi t}\, e^{\,-t/T2^*} \,|\, A(G_b,t) \,| \qquad [1]$$

where w and f are the magnitude of water and fat signals, Δf is the chemical shift difference between fat and water, ψ is the B_0 inhomogeneity, $A(t)$ is the time profile of the excitation pulse, and G_b is the linear background gradient in the slice selection direction. A major assumption of this model is that the T_2* relaxations are the same for water and fat. This may be resonable when T_2* decay is dominated by the presence of iron and fat fraction is relatively small (8, 15). Assuming that phase dispersion and magnitude decay due to G_b are identical for water and fat, the additional signal decay related to the background

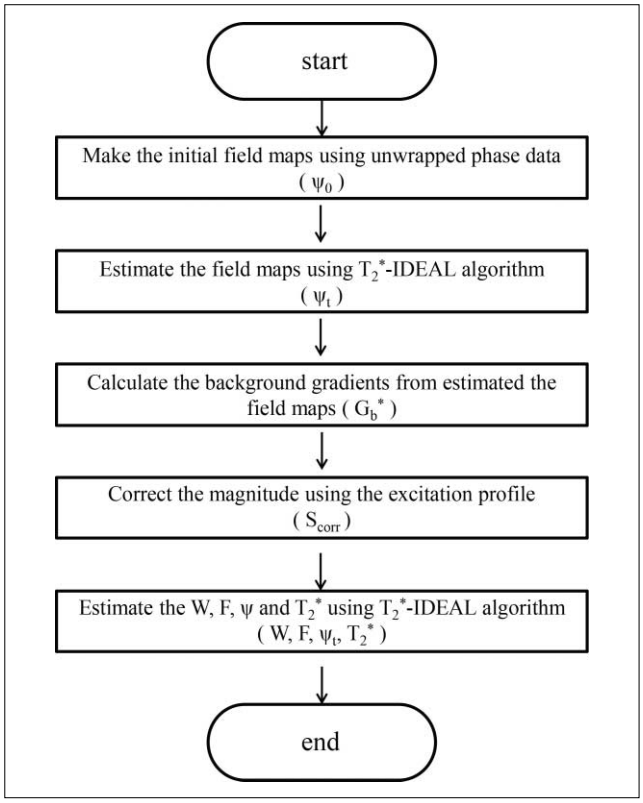

Fig. 1. Flow chart of the proposed background gradient correction algorithm for quantification of fat, water and T_2*. The output variables of each step are given in brackets.

gradient can be corrected by estimating the G_b values if the excitation pulse profile is given (12).

Background Gradient Correction and T_2*-IDEAL

The B_0 field inhomogeneity (ψ) should first be calculated to estimate the background gradients (G_b) which correct for the signal decay. In a multi-slice scan, G_b can be approximated by linear fitting of ψ in the slice-select direction at each voxel from the phase information of adjacent slices (13). T_2*-IDEAL algorithm provides the B_0 field inhomogeneities at each voxel along with the fat content, water content, and the T_2* values by complex data fitting (8). However, an incorrect ψ can be estimated from T_2*-IDEAL when the field inhomogeneity is severe. For example, if the estimated ψ is closer to $\psi_t + \Delta f$ (ψ_t is the real ψ), T_2*-IDEAL can result in swapped water and fat signals (16). Therefore, here, the initial field map was calculated from the two unwrapped phase images to prevent false convergence. Two echoes which have similar phase with respect to Δf were chosen for the initial field map to minimize the contamination caused by the chemical shift of water and fat. Phase unwrapping was conducted by applying the automatic phase unwraping algorithm, PRELUDE (17). The B_0 field inhomogeneities (ψ) derived from T_2*-IDEAL were then used for background gradient estimation at each voxel:

$$G_b^* = ((\psi_n + 1 - \psi_n) \Delta z) / (\gamma (\Delta z + \Delta d)) \quad [2]$$

where ψ_n is the B_0 field inhomogeneity of the nth slice, γ is the gyromagnetic ratio, Δz is the slice thickness, and Δd is the slice gap.

To minimize the elimination of the effect of the non-macroscopic field inhomogeneities, 2D median filtering was conducted to the calculated background gradient (G_b) maps in the each slice. Afterwards, a pixelwise magnitude correction of the signal is performed by dividing the excitation pulse profile for all echoes:

$$s_{corr}(t) = s(t) / | A(G_b^*, t) | \quad [3]$$

where $s_{corr}(t)$ is the corrected signal for data at t and G_b* is the estimated linear background gradient.

Generally, a sinc weighted correction algorithm is used which assumed a perfect rectangular slice profile (12, 13). However, a weighting function induced by linear background gradient is not exactly a sinc function when, e.g., windowing is used to achieve a better excitation profile. If a hanning windowed sinc was used for slice selective excitation, then the theoretical weighting function would be

$$A(G_b, t) = 0.5\ sinc(\gamma G_b\ t)\ (1 + cos(\pi \gamma G_b\ t)) \quad [4]$$

Note that this also depends on the flip angle. Finally, the water content, fat content and T_2* were recalcu-

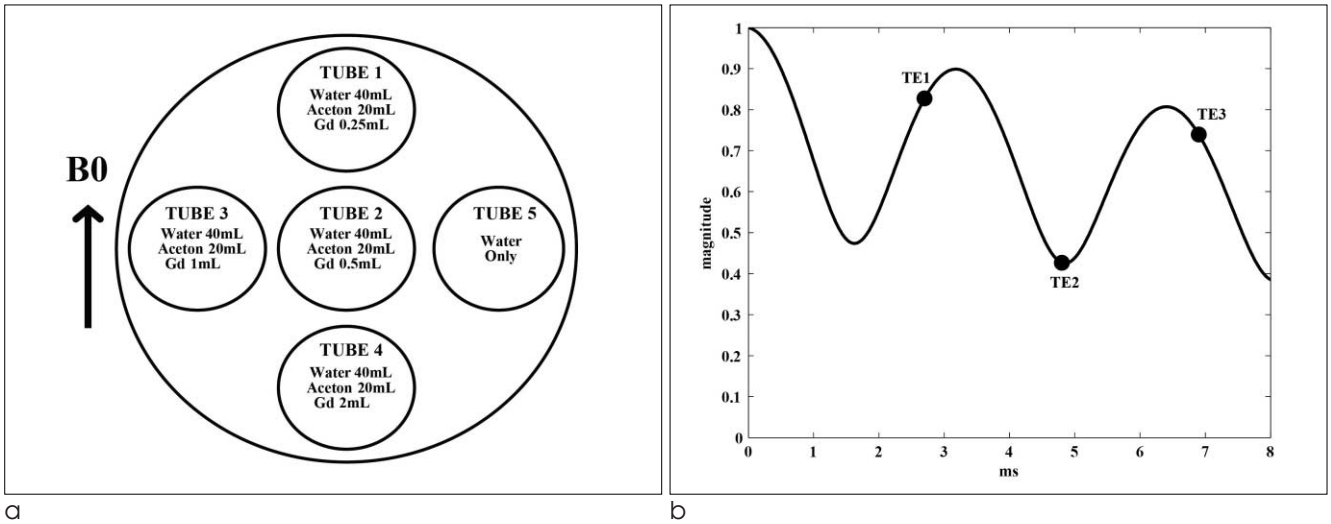

a b

Fig. 2. a. The composition of the water and aceton phantom used in this study. Four tubes contain the same volume of water and aceton but different Gd concentrations. b. The signal model of water and aceton determined by –310 Hz chemical shift. The acquired three echoes are pointed by circles.

lated by T_2*-IDEAL algorithm from the corrected signal $S_{corr}(t)$. A summary of the overall processing is described in Fig. 1. All processing used in this study was done in MATLAB (The MathWorks, Natwick, MA).

MRI Experiments

To examine the validity of the weighting function used for magnitude correction, the actual excitation profiles followed by the applied RF pulses were measured for various flip angles. The identical Hanning windowed sinc pulses were applied to the same scanner used in the phantom and in vivo experiments. The excitation profiles were simply measured by applying the readout gradients in the slice-selection direction without any other directional gradients (Fig. 3). The excitation profiles for five different flip angles (10°, 20°, 30°, 40°, 50°) were measured with identical slice thickness (5 mm) in the phantom experiments.

To examine the effect of the background gradient in the slice-selection direction on the results of T_2*-IDEAL algorithm, phantom studies were performed. Because fat is not soluble in water, aceton was used as an alternative to fat. Gadolinium (Gd) contrast agent of 0.5 mol/L concentration (Dotarem, Guerbet, France) was used to make different T_2* values induced by susceptibility differences. The chemical shift between acetone and water was determined to be −310 Hz by spectroscopy. Four tubes were constructed with the same amount of water and aceton volume, but different Gd volumes (0.25 mL, 0.5 mL, 1 mL, 2 mL). One tube was constructed with only water for reference. Figure 2 illustrates the phantom used in this study. Three different linear background gradients in the slice-selection direction were applied by adjusting the manual shim of the scanner. Imaging was performed by 3 T (Siemens Tim Trio, Erlangen, Germany) using a multi-echo 2D spoiled gradient echo pulse sequence. The Hanning windowed sinc pulse was used for the slice selective excitation. Imaging parameters were as follows: TE = 2.7 ms, 4.8 ms, 6.9 ms, ΔTE = 2.1 ms ($\theta i = 2\pi/3$), TR = 500 ms, flip angle = 20°, bandwidth = 1502 Hz/px, voxel size = $1.8 \times 1.8 \times 5.0$ mm^3, matrix size = 128×128, 16 interleaved slices with a gap of 2.5 mm, number of averages = 4, applied G_b in the slice-selection direction = 0 μT/m, 50 μT/m, 100 μT/m.

In vivo imaging was performed on two healthy volunteers under the approval of the local institutional review board. Twelve transverse slices were obtained using a multi-echo 2D gradient echo pulse sequence on the same scanner. The chemical shift between fat and water used for T_2*-IDEAL was assumed to be 420 Hz. Imaging parameters were as follows: Hanning windowed sinc RF (duration = 1 ms), six echoes acquired at TE = 2.1, 3.6, 5.1, 6.6, 8.1, 9.6 ms ($\theta i = 4\pi/3$), TR= 132 ms, flip angle=20°, voxel size = $2.5 \times 2.5 \times 8$ mm^3, matrix size = 128×128, 12 interleaved slices with a gap of 4 mm, bandwidth = 1502 Hz/px, total scan time = 16.89 s with breath holds.

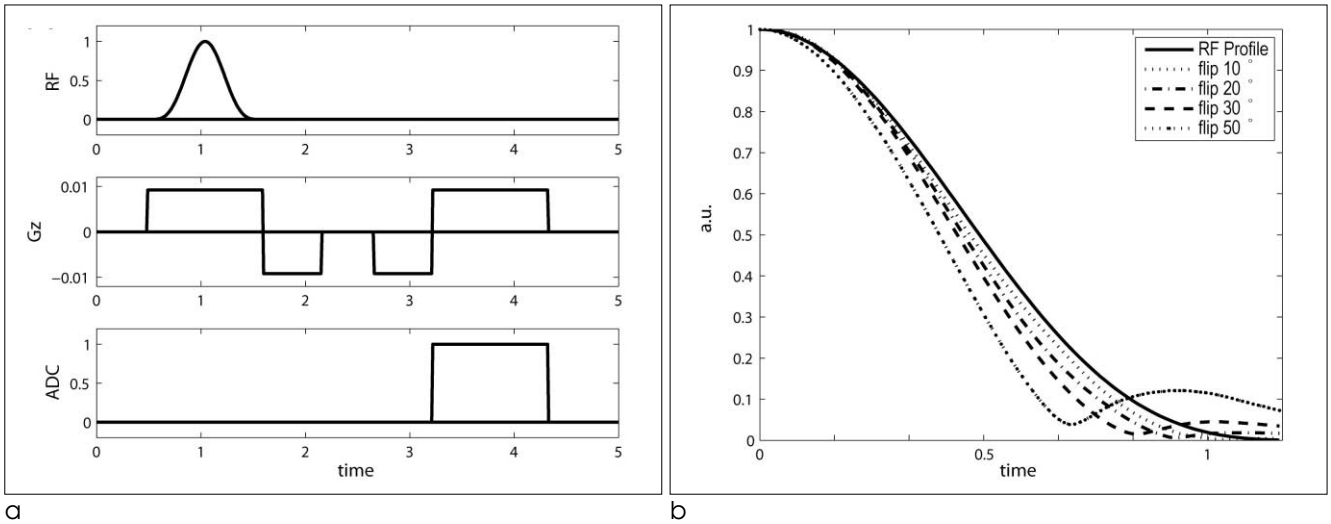

a b

Fig. 3. a. Pulse diagram used to obtain the actual excitation profile. b. The applied excitation pulse profile and the measured excitation profiles for different flip angles.

RESULTS

Figure 3 shows the applied excitation pulse profile and the measured excitation profiles for different flip angles. The measured excitation profiles show very similar shape with the applied excitation pulse profile for small flip angles less than 30°. Although the measured excitation profiles decay faster and zero crossing points appear as the flip angles increase, it is not a problem at the flip angle of 20° used in this study. Note that the faster decay in the measured profile compared to actual profile comes also from transverse magnetization decay.

Figure 4 shows the estimated linear background gradient, T_2* and aceton fraction maps from the phantom experiments. The estimated linear background gradients (G_b) are in good agreement with the actual applied G_b values. While the T_2* values changed by applying the linear background gradients, the aceton fractions changed very slightly. In the first row (well-shimmed condition), the aceton fractions are larger and the T_2* values are shorter at the higher Gd concentrations. The uncorrected T_2* values in the second and third row (artificial 50 μT/m and 100 μT/m background gradients added in the slice-selection direction) are shorter than the well-shimmed condition as the linear background gradients are increased. The corrected T_2* values in the second and third row show similar T_2* values to those of the well-shimmed condition. However, the aceton fractions in each tube are very slightly changed as compared to the well-

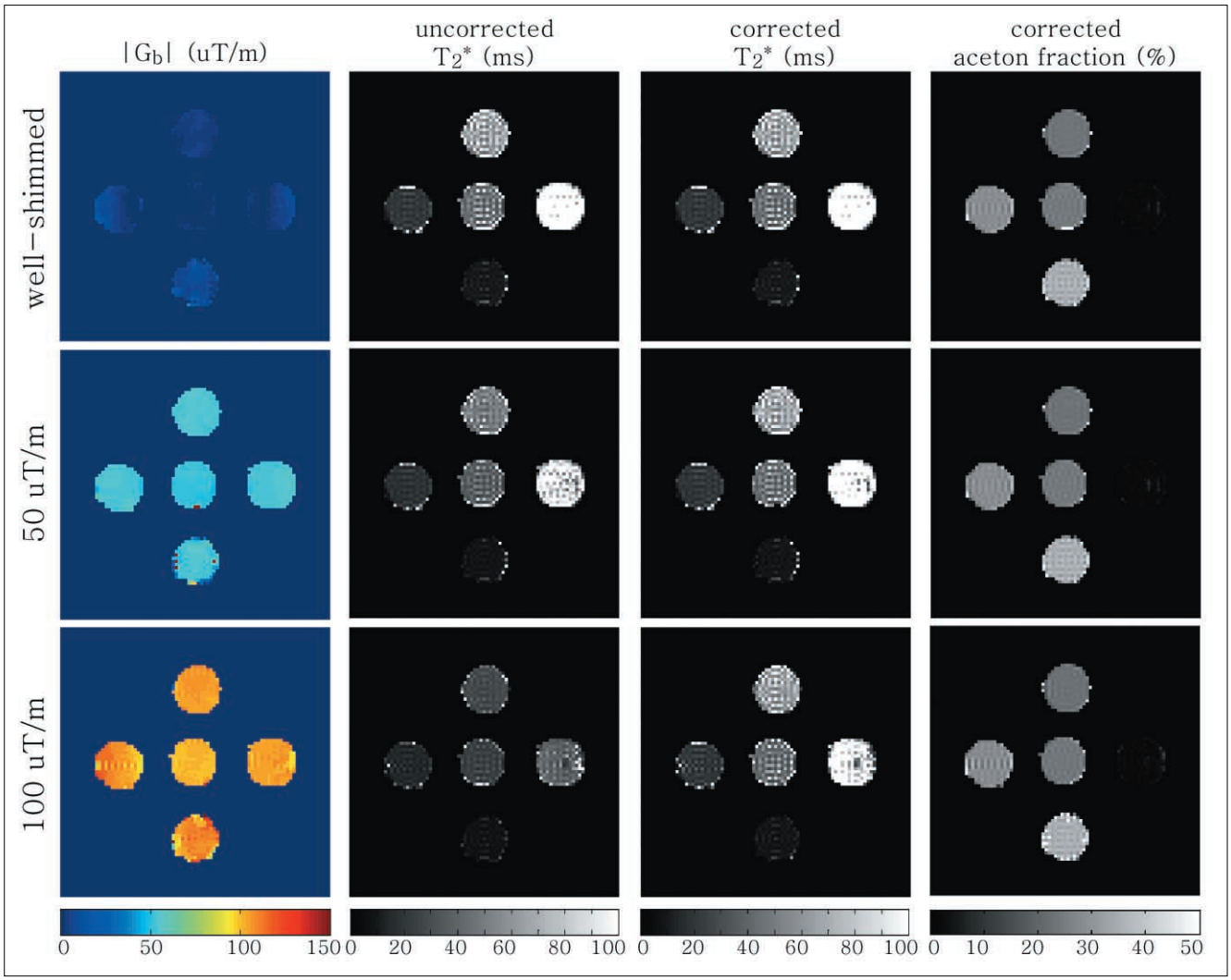

Fig. 4. Results from the water and aceton phantom scans with a spatial resolution of 1.8 × 1.8 × 5.0 mm³.
The estimated linear background gradient (G_b), T_2* and aceton fraction maps for different shim conditions.

shimmed condition. Table 1 shows the numerical results calculated from 60 voxels in each tube. The average ratios of the estimated T_2* values to the well-shimmed condition changed from 0.82 to 0.95 for background gradient of 50 uT/m and from 0.61 to 0.96 for that of 100 uT/m with the correction method. The average ratios of the estimated aceton fraction changed from 0.99 to 1.00 for 50 μT/m and from 0.98 to 0.99 for 100 μT/m.

Figure 5 shows in vivo liver imaging results of the linear background gradient, fat fraction and T_2* maps. The calculated G_b map shows large values (up to about 120 μT/m) on the lower-left regions of liver and the uncorrected T_2* values of this region are relatively short. The corrected fat fractions, in common with the results from phantom experiments, are similar to the uncorrected fat fractions. Two regions of interest containing 50 voxels were manually selected for each subjects (circle in Fig. 5) to investigate the effect of linear background gradients. The mean G_b of the ROI 2 is larger than the ROI 1 and the uncorrected mean T_2* of the ROI 2 is shorter than that of the ROI 1 (ROI 2: 15.6, ROI 1: 19.9 for subject 1 and ROI 2: 12.7, ROI 1: 20.5 for subject 2). However, the corrected mean T_2* of the ROI 2 is similar to that of ROI 1 (ROI 2: 22.8, ROI 1: 24.1 for subject 1 and ROI 2: 21.3, ROI 1: 24.9 for subject 2) and the ratio of the ROI 2 and ROI 1 changed from 0.78 to 0.95 for subject 1 and 0.62 to 0.91 for subject 2. Table 2 shows the estimated G_b, fat fraction, T_2* values from ROI 1 and ROI 2.

DISCUSSION

In this study, we have applied the correction method for background gradients in slice-selection direction to T_2*-IDEAL for 2D liver imaging. The proposed method can be helpful for more accurate T_2* quantification in liver by separating the additional signal decay induced by macroscopic field inhomogeneities from the decay caused by iron. It is difficult to ignore the additional signal decay due to background gradients in the slice-selection direction reducing the slice thickness can have problems in covering the whole 3D volume in a single breath-hold. The fat fraction, however, calculated by T_2*-IDEAL did not change significantly after applying correction methods. Assuming the effect of macroscopic field inhomogeneity is identical to water and fat, this result is resonable because the correction algorithm only corrects magitude information.

Using an excitation pulse profile for magnitude correction is an essential part of this study but its limitation should also be considered. It is correct that signal decay due to a linear background gradient is weighted by an excitation pulse shape under the assumption of Fourier relationship between the excitation pulse and slice profile. However, this assumption is derived from the Bloch equation when the flip angle

Table 1. The estimated mean±standard deviation of aceton fraction and T_2* of 4 tubes before and after applying the correction method for different shim conditions. The numbers in the brackets are the ratio to the uncorrected well-shimmed condition. Bold numbers indicate the corrected values after applying the proposed algorithm

		Tube1	Tube2	Tube3	Tube4
Well-shimmed condition	Aceton (%)	23.24 ± 0.34 (1.00) → **23.24 ± 0.34 (1.00)**	24.49 ± 0.67 (1.00) → **24.49 ± 0.67 (1.00)**	28.27 ± 1.08 (1.00) → **28.27 ± 1.08 (1.00)**	35.13 ± 1.31 (1.00) → **35.09 ± 1.27 (1.00)**
	T_2* (ms)	64.4 ± 11.3 (1.00) → **64.5 ± 11.3 (1.00)**	45.5 ± 9.3 (1.00) → **45.5 ± 9.3 (1.00)**	19.7 ± 2.1 (1.00) → **19.8 ± 2.1 (1.01)**	10.0 ± 1.1 (1.00) → **10.0 ± 1.1 (1.00)**
50 uT/m	Aceton (%)	22.98 ± 0.35 (0.98) → **23.05 ± 0.35 (0.99)**	24.31 ± 0.66 (0.99) → **24.37 ± 0.66 (1.00)**	28.19 ± 1.02 (1.00) → **28.24 ± 1.02 (1.00)**	35.17 ± 1.19 (1.00) → **35.26 ± 1.24 (1.00)**
	T_2* (ms)	47.9 ± 5.3 (0.74) → **63.5 ± 9.6 (0.98)**	37.3 ± 6.3 (0.82) → **45.1 ± 9.4 (0.99)**	17.5 ± 1.8 (0.89) → **19.2 ± 2.2 (0.97)**	8.3 ± 0.9 (0.83) → **8.7 ± 0.9 (0.87)**
100 uT/m	Aceton (%)	22.64 ± 0.44 (0.97) → **22.87 ± 0.43 (0.98)**	23.98 ± 0.64 (0.98) → **24.21 ± 0.63 (0.99)**	27.73 ± 1.58 (0.98) → **27.95 ± 1.56 (0.99)**	34.89 ± 1.17 (0.99) → **35.05 ± 1.18 (1.00)**
	T_2* (ms)	27.7 ± 2.0 (0.43) → **62.9 ± 10.3 (0.98)**	24.1 ± 2.6 (0.53) → **43.8 ± 8.6 (0.96)**	14.0 ± 1.6 (0.71) → **19.7 ± 3.2 (1.00)**	7.5 ± 1.2 (0.75) → **8.9 ± 1.5 (0.89)**

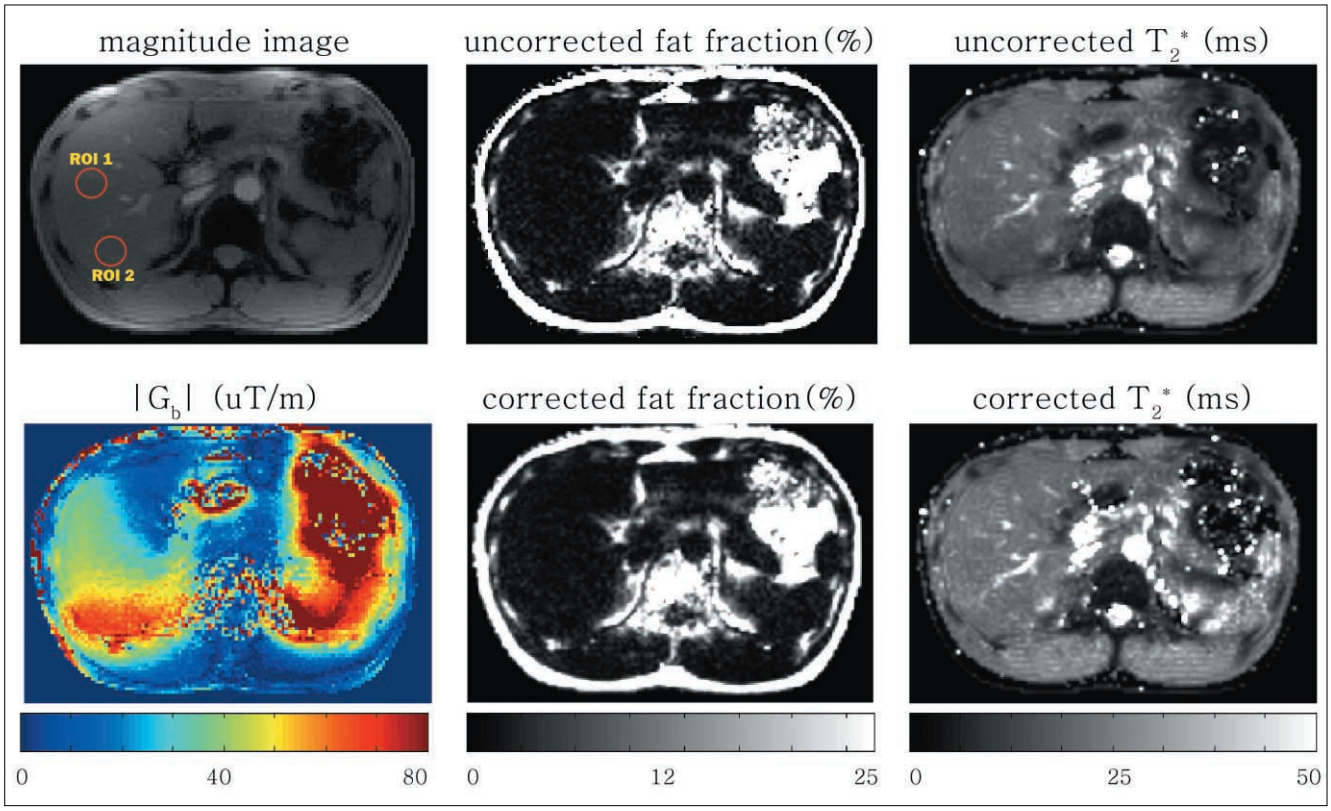

a

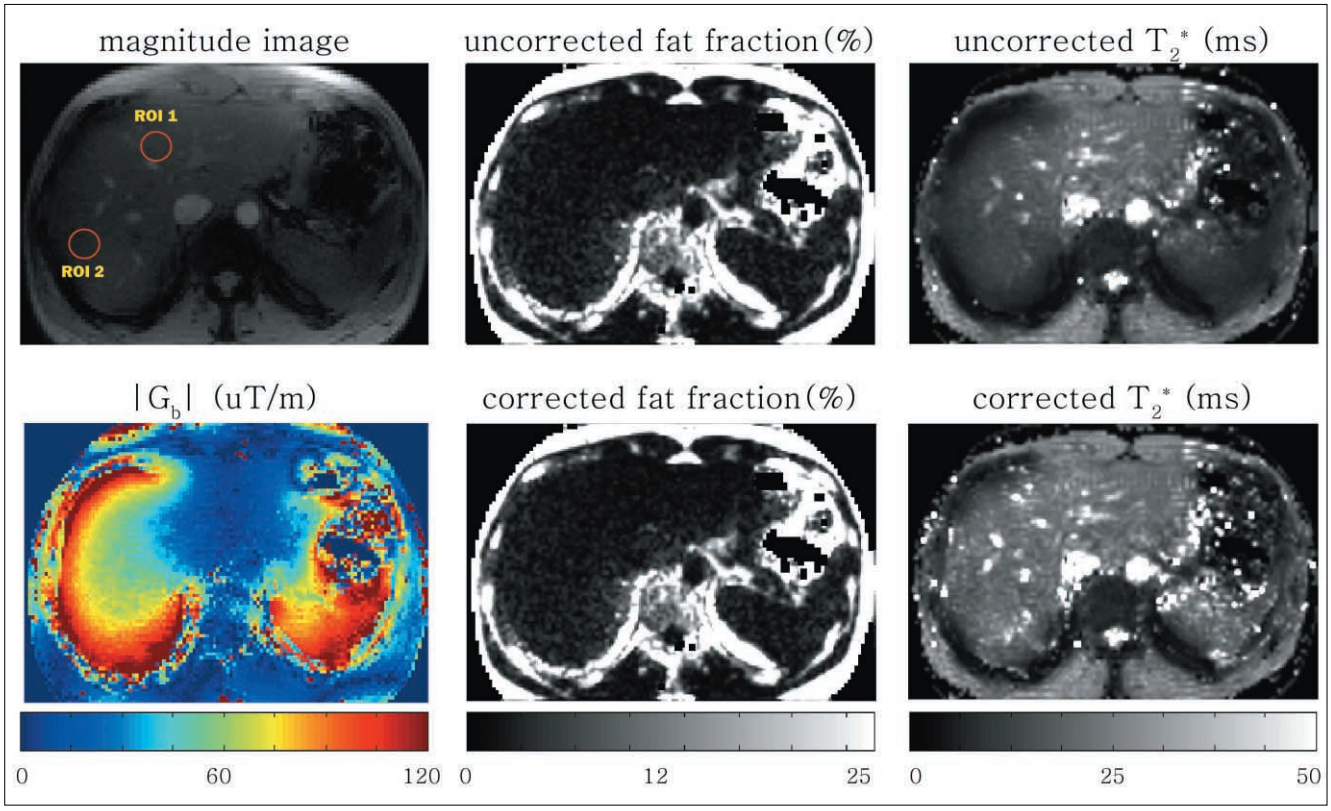

b

Fig. 5. Results from two healthy volunteers (a, b**) with a spatial resolution of 2.5 × 2.5 × 8.0 mm³.** 5th echo (8.1 ms) magnitude image and its estimated linear background gradient (G_b) , fat fraction and T_2* maps.

Table 2. The estimated mean±standard deviation of G_b, fat fraction and T_2* from ROI 1 and ROI 2 of two subjects (Fig. 5). Arrow indicates the uncorrected (the left side of the arrow) and the corrected (the right side of the arrow) values by the proposed algorithm

	ROI 1	ROI 2	RATIO (ROI2/ROI1)
		Subject 1	
Gb (uT/m)	39.07±1.68	58.99±4.00	1.51
Fat (%) Uncorrected → Corrected	1.91±0.99 → 1.96±1.02	1.76±0.81 → 1.84±0.82	0.92 → 0.94
T_2*(ms) Uncorrected → Corrected	19.9±2.5 → 24.1±3.8	15.6±1.3 → 22.8±3.3	0.78 → 0.95
		Subject 2	
Gb (uT/m)	30.91±4.32	61.42±5.91	1.99
Fat (%) Uncorrected → Corrected	1.68±0.71 → 1.76±0.74	2.45±1.17 → 2.58±1.14	1.46 → 1.47
T_2*(ms) Uncorrected → Corrected	20.5±4.1 → 24.9±4.6	12.7±1.7 → 21.3±3.5	0.62 → 0.91

is sufficiently low. As seen in Fig. 3, the disagreement between the actual profile and the applied profile becomes larger as the applied flip angle increase. Therefore, the effect of transmit RF field inhomogeneity should be considered when a large flip angle is used. In addition, when the object is nonuniform through-slice, the signal is not simply multiplied by the excitation pulse profile. But, rather the spatial-frequency components of the slice are convolved with Fourier transform of the excitation profile. This is not a practical problem in most liver imaging because a low flip angle is typically used for minimizing T_1 effects and slice structure does not prevail. However, it should be also considered for more accurate quantification, especially when a large flip angle is used.

B_0 field map (ψ) estimation in each slice is also an important step in obtaining accurate linear background gradients. When the field inhomogeneity exceeds the maximum frequency determined by echo spacing, phase wrapping occurs. As a result, an incorrect ψ was estimated in T_2*-IDEAL algorithm when the initial ψ_0 is inappropriate. In this study, a phase unwrapping algorithm was used to obtain the initial field map close to the true field map. While this may reduce an incorrect convergence of T_2*-IDEAL, it is complex to implement and time consuming. To resolve these problems, other field map estimation methods such as a region growing method (16), a multiresolution method (18) can be used for efficient quantification.

In our phantom experiments, fat fractions are large at higher Gd concentrations although the actual fat fractions of all the tubes were the same. We suspect that the increased fat fraction at higher Gd concentration is related to the signal model used for quantification. A recent study regarding signal models for fat quantification using SPIO showed similar results when the signal model assumed identical T_2* between water and fat (15, 19). However, the fat fraction didn't increase much at higher SPIO concentration in the signal model which has independent T_2* of water and fat (15). They guessed that SPIOs preferentially accelerate the signal decay of water more than that of fat because water and fat have different solubilities, so the fat fraction is overestimated at higher SPIO concentrations. Accordingly, independent estimation of T_2* of water and fat will be needed when iron overload is severe. However, the independent T_2* estimation remarkably increases the complexity of the algorithm and computing time (15).

In conclusion, this study investigated the effect of background gradient in the slice-selection direction

and demonstrated a correction method using excitation pulse profile for simultaneous fat and T_2* quantification in 2D multi-slice liver imaging. It is anticipated that this correction method will be helpful for the quantification of fat and T_2* in the presence of macroscopic field inhomogeneity.

Acknowledgements:

This study was supported by a grant of the Korean Health Technology R&D Project, Ministry for Health, Welfare & Family Affairs, Republic of Korea (A110035-1101-0000200).

References

1. Hussain HK, Chenevert TL, Londy FJ, et al. Hepatic fat fraction: MR imaging for quantitative measurement and display--early experience. Radiology 2005;237:1048-1055
2. Park H, Cho H, Kim E, Hur G, Kim Y, Lee B. Detection of hepatic lesion: comparison of free-breathing and respiratory-triggered diffusion-weighted MR imaging on 1.5-T MR system. J Korean Soc Magn Reson Med 2011;15:22-31
3. Dixon WT. Simple proton spectroscopic imaging. Radiology 1984;153:189-194
4. Glover GH, Schneider E. Three-point Dixon technique for true water/fat decomposition with B0 inhomogeneity correction. Magn Reson Med 1991;18:371-383
5. Wood JC, Enriquez C, Ghugre N, et al. MRI R2 and R2* mapping accurately estimates hepatic iron concentration in transfusion-dependent thalassemia and sickle cell disease patients. Blood 2005;106:1460-1465
6. O'Regan DP, Callaghan MF, Wylezinska-Arridge M, et al. Liver fat content and T_2*: simultaneous measurement by using breath-hold multiecho MR imaging at 3.0 T--feasibility. Radiology 2008;247:550-557
7. Reeder SB, Pineda AR, Wen Z, et al. Iterative decomposition of water and fat with echo asymmetry and least-squares estimation (IDEAL): application with fast spin-echo imaging. Magn Reson Med 2005;54:636-644
8. Yu H, McKenzie CA, Shimakawa A, et al. Multiecho reconstruction for simultaneous water-fat decomposition and T_2* estimation. J Magn Reson Imaging 2007;26:1153-1161
9. Haacke EM, Tkach JA, Parrish TB. Reduction of T2* dephasing in gradient field-echo imaging. Radiology 1989;170:457-462
10. Cho S, Kim P, Lim J, Ahn C. Model-based Gradient Compensation in Spiral Imaging. J Korean Soc Magn Reson Med 2009;13:15-21
11. Cho ZH, Ro YM. Reduction of susceptibility artifact in gradient-echo imaging. Magn Reson Med 1992;23:193-200
12. Fernandez-Seara MA, Wehrli FW. Postprocessing technique to correct for background gradients in image-based R*(2) measurements. Magn Reson Med 2000;44:358-366
13. Dahnke H, Schaeffter T. Limits of detection of SPIO at 3.0 T using T2 relaxometry. Magn Reson Med 2005;53:1202-1206
14. Pauly JM. New approach to selective excitation for magnetic resonance imaging. Doctral Thesis, Stanford University 1990
15. Chebrolu VV, Hines CD, Yu H, et al. Independent estimation of T*2 for water and fat for improved accuracy of fat quantification. Magn Reson Med 2010;63:849-857
16. Yu H, Reeder SB, Shimakawa A, Brittain JH, Pelc NJ. Field map estimation with a region growing scheme for iterative 3-point water-fat decomposition. Magn Reson Med 2005;54:1032-1039
17. Jenkinson M. Fast, automated, N-dimensional phase-unwrapping algorithm. Magn Reson Med 2003;49:193-197
18. Lu W, Hargreaves BA. Multiresolution field map estimation using golden section search for water-fat separation. Magn Reson Med 2008;60:236-244
19. Bydder M, Shiehmorteza M, Yokoo T, et al. Assessment of liver fat quantification in the presence of iron. Magn Reson Imaging 2010;28:767-776

대한자기공명의과학회지 16:6-15(2012)

불균일 자장 보정 후처리 기법을 이용한 간 영상에서의 지방 및 T_2* 측정

[1]연세대학교 전기전자공학과
[2]연세대학교 의과대학 영상의학과

남윤호[1] · 김한성[1] · 조상영[1] · 김동현[1, 2]

목적: 이 연구의 목적은 excitation pulse profile을 이용하여 불균일 자장에 의하여 발생하는 배경 경사 자장에 의한 영향을 보상하여 2차원 다중 단면 경사에코 간 영상에서의 정확한 지방 및 T_2* 측정을 하는 데에 있다.

대상과 방법: 2차원 경사에코영상에서 불균일 자장에 의한 배경경사자장으로 인하여 유도되는 신호의 감소는 excitation pulse profile weighting으로 나타난다. 이에 의한 영향을 최소화 하기 위하여 B_0 field map을 통하여 단면선택방향으로의 선형 경사자장의 정도를 추정한 후, 획득한 신호를 excitation pulse profile을 이용하여 보정하였다. T_2* 및 지방은 보정된 신호로부터 측정되었으며 보정방법은 3.0T 임상용 장비에서 팬텀 및 in vivo 실험을 통하여 이루어 졌다.

결과: 팬텀 실험 결과는 보정 후 측정된 T_2* 및 지방의 양이 자장이 균일한 경우에 가까워 진 것을 보여 주었다. In vivo 실험에서는 간에서 배경경사자장의 크기가 약 120 μT/m 정도 까지로 나타났으며 보정하기 전에 비하여 측정된 T_2* 및 지방의 정도의 균일도가 높아지는 것을 확인할 수 있었다.

결론: Excitation pulse profile을 이용한 배경경사자장 보정 방법은 경사 에코 신호에서의 거시적인 불균일 자장에 의한 영향을 줄여 주며 2차원 간 영상에서의 적용을 통하여 보다 정확한 지방 및 T_2*의 측정에 도움이 될 수 있다.

통신저자 : 김동현, (120-749) 서울특별시 서대문구 신촌동 134, 연세대학교 전기전자공학과
Tel. (02) 2123-5874 Fax. (02) 313-2879 E-mail: donghyunkim@yonsei.ac.kr